Sweep measurements of the transfern function of a RF-channel and its representation by polynominals

Autor(en): **Liniger, Markus**

Objekttyp: **Article**

Zeitschrift: **Technische Mitteilungen / Schweizerische Post-, Telefon- und Telegrafenbetriebe = Bulletin technique / Entreprise des postes, téléphones et télégraphes suisses = Bollettino tecnico / Azienda delle poste, dei telefoni e dei telegrafi svizzeri**

Band (Jahr): **60 (1982)**

Heft 7

PDF erstellt am: **11.07.2024**

Persistenter Link: https://doi.org/10.5169/seals-876167

Sweep Measurements of the Transfer Function of a RF-Channel and its Representation by Polynomials

Markus LINIGER, Berne

621.371.31.029.64:621.391.812.3.029.64

1 Introduction

The introduction of high-capacity digital radio links has revealed that the propagation statistics collected for FM-FDM-transmission over line-of-sight radios are insufficient for the new requirements. So far most investigations were performed with CW-signals. These have to be supplemented by measurements in a sufficiently broad RF-channel. Therefore, the Swiss PTT Administration decided to perform swept recordings on several hops of the national radio-link network.

A measurement bandwidth of 40 MHz was selected. This has the advantage that within a rather short time period several hops can be investigated by use of the existing infrastructure. But it severely limits the possibility to separate two signals with a relatively small difference in path length. However, this disadvantage is not important, if real or complex polynomials with time-dependent coefficients are used for the description of the channel model. The remaining problem to be solved is the combination of the channel model with characteristics of the radio-link equipment which may typically be described by the signature [1, 2]. One approach to this problem consists in transforming the signature into the expanded (by one dimension) finite polynomial space. This transformed signature can then be treated in the same space as the channel model.

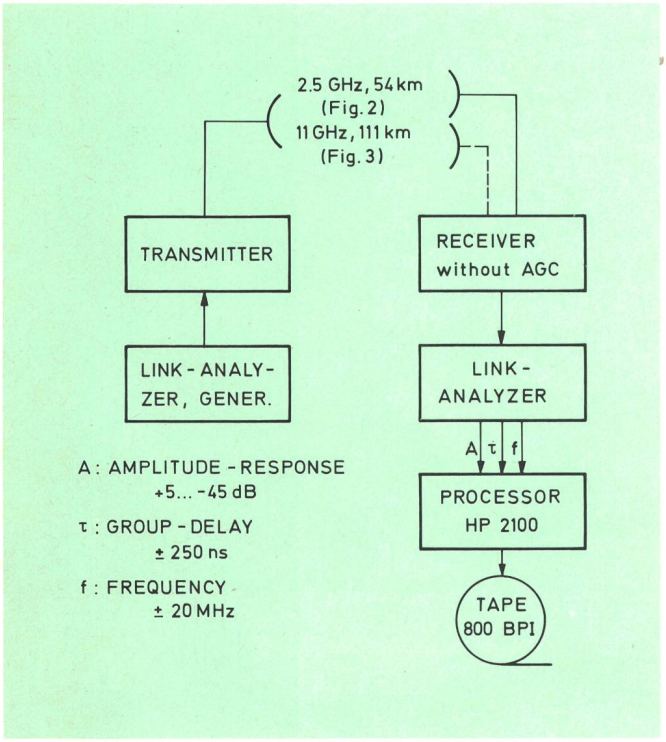

Fig. 1
Measurement equipment

2 Measurement system, data aquisition and processing

The measurement system consists of the RF-part of a FM radio link and a link analyzer RM-4 (Wandel + Goltermann), as shown in *figure 1*. After a few minor modifications, the analyzer fulfilled the following specifications:

Sweep frequency	5 Hz
Amplitude range	+5 . . . −45 dB
Group delay range	±250 ns

The three measured analogue quantities, namely sweep voltage (corresponding to frequency), amplitude and group delay are digitized and preprocessed by the processor HP 2100. Two types of statistics are collected, long-term and short-term. Values for the long term statistics are taken every 15 s and stored on magnetic tape. They consist of the results of an entire swept measurement as well as extreme and average values for the previous 15 second interval. If the variations of the measured values exceed given limits or if the amplitude falls below a given value, then the raw data are stored in addition to the long term values. By means of this strategy a magnetic tape suffices for a recording period between 10 hours to 25 days depending on the fading activity.

The information stored on magnetic tape is subsequently processed in the computer center of the PTT, where erroneous data are deleted based on plausibility tests and additional input from an analogue paper registration which operated in parallel to the computer data collection system. The cleaned-up data are then separated into long-term and short-term registrations.

Any further processing is done in the batch mode with FORTRAN programs which prepare important intermediate results for access by APL.

3 Description of the measured hops

The first hop measured has a length of 54 km and was selected because of its large path clearance *(fig. 2)*. It was our intent to observe interfering rays with detours as large as possible and thus to find an upper limit for the delay τ. For our measurements an 1800-channel system operating at 2472 MHz was available. Two circular parabolic antennas with a diameter of 4.3 m were employed.

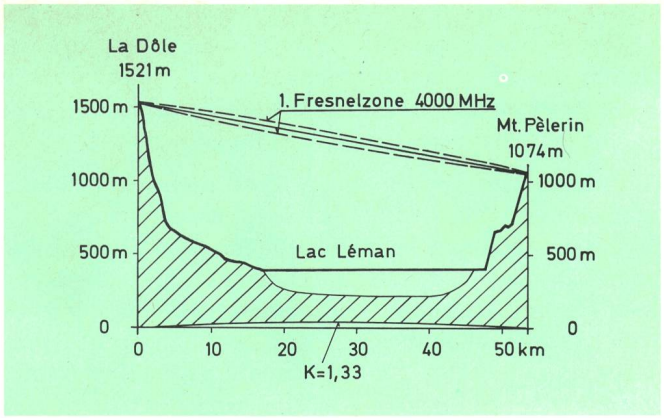

Fig. 2
Profile La Dôle—Mt-Pèlerin

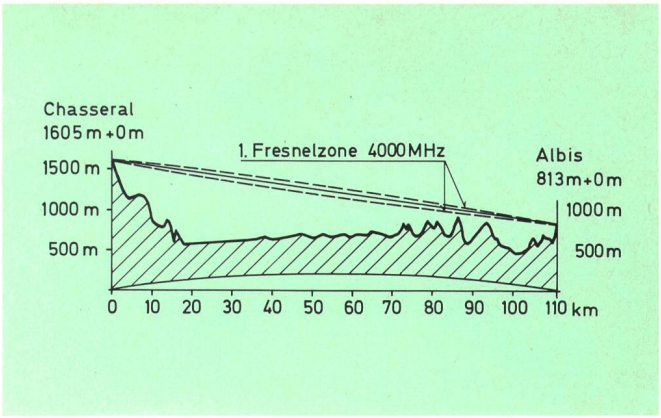

Fig. 3
Profile Chasseral-Albis

The second experiment was conducted on a hop of 111 km length and at 11.285 GHz *(fig. 3)*. The transmit antenna was a circular parabolic dish of 4.3 m diameter. On the receive side two offset-parabolic antennas (type CM 4671 by Thomson CSF) with a diameter of 4 m were used. Their vertical separation was 11.8 m. This allowed to study the influence of space-diversity reception. The two receive signals were added with an electronic RF-combiner [3]. During the measurements the diversity path was switched in and out at hourly intervals. In addition, provisions were made to receive also the cross-polarized signal in order to study its influence at frequency separations between 0 and 40 MHz.

4 Measurement results

In order to get a better overview over the huge amount of data, three-dimensional drawings of particular events were made. The amplitude and group delay are plotted as functions of time and frequency.

41 La Dôle—Mt-Pèlerin, d = 54 km, f = 2.5 GHz

Figure 4 shows a sample of the amplitude of the 2.5 GHz-receive signal as measured on the hop according to figure 2. The periodic behavior of the response is noteworthy. It clearly indicates the presence of a second signal with a delay of 110 ns. The analysis of the profile (Fig. 2) and of the antenna diagrams prove conclusively that the second propagation path originates from reflections from the lake of Geneva. The received amplitude of this signal is in good agreement with the reflection coefficient of the lake ($r \approx 0.9$) and the attenuation due to the antenna diagrams (6 dB and 13 dB, respectively). During a second experimental phase both antennas were tilted upward by approximately 0.7° which resulted in 1 dB loss for the direct ray but 15 dB loss for the reflected ray. The result was as expected. The transfer function remained unchanged in shape, but shifted to lower signal values by 15 dB.

For both measurement periods the transfer function can be approximated by a three-ray model [4],

$$H(s) = 1 + a_2 \exp(-s\tau_2) + a_3 \exp(-s\tau_3)$$

with

$$\tau_2 \leqq 2\text{ ns} \ll \tau_3 = 110\text{ ns}$$

Despite a very large path clearance in the «direct» path, no large delay values for τ_2 were observed.

42 Chasseral—Albis, d = 111 km, f = 11 GHz

The measurements on the 11 GHz hop were started in March 1981. During the first seven weeks the transfer function was measured without space-diversity protection. Two selected examples demonstrate that flat fadings *(fig. 5)* well as fadings with selective attenuation

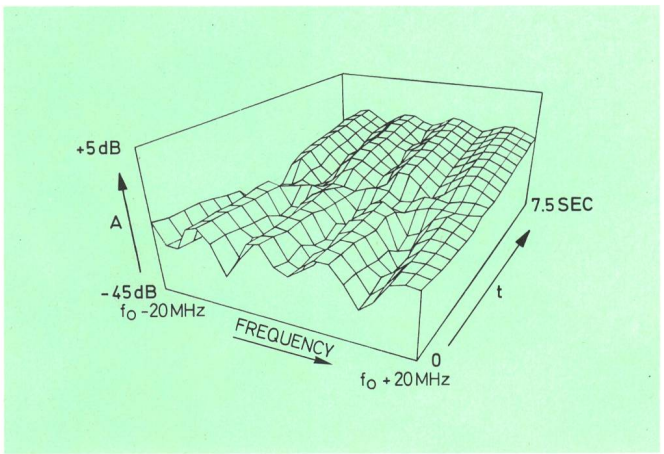

Fig. 4
Example of a multipath fading La Dôle—Mt-Pèlerin, 2.5 GHz, d = 54 km

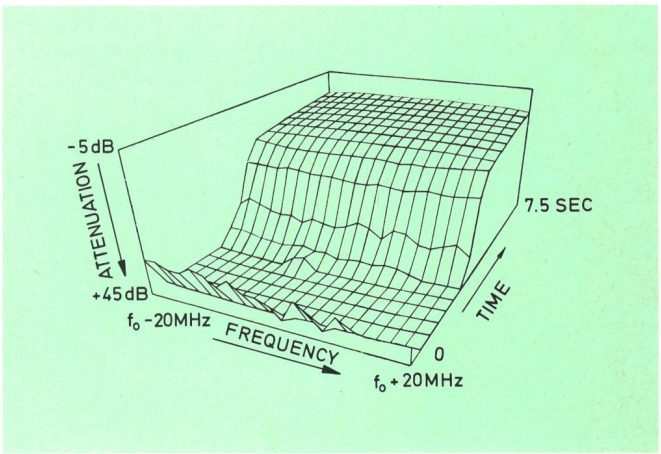

Fig. 5
Example of a flat multipath fading Chasseral—Albis, 11 GHz, d = 111 km

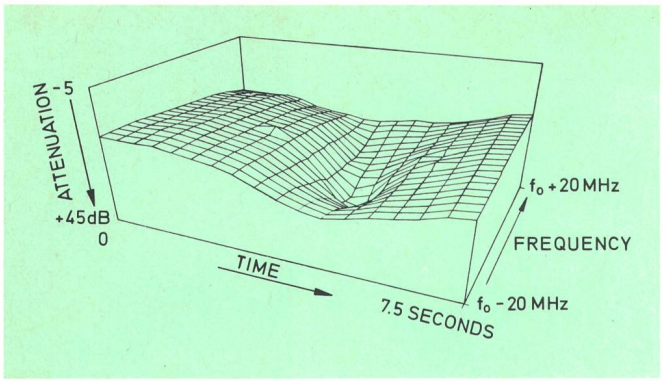

Fig. 6
Example of a selective multipath fading Chasseral—Albis, 11 GHz, d = 111 km

(fig. 6) do occur. But generally, all fadings on this path are much less severe than those on the hop La Dôle—Mt-Pèlerin as far as the frequency selectivity is concerned.

During a second period (June—December 81) the space-diversity combiner was switched in and out in hourly intervals under the control of the measurement processor. These measurement intervals were chosen in such a way that periods with known frequent fadings — they usually last 4 to 6 hours — are evenly distributed among both receiving techniques. This ensures that the statistics are representative for both cases.

Any unavoidable differences in the transfer functions of the equipment involved are taken into account by calibrating the system with and without diversity system during periods of undisturbed propagation. The resulting calibration curves serve to correct each individual swept measurement so that subsequent corrected results can be compared directly with each other. Hence an attenuation of 0 dB means in every case 0 dB with respect to the undisturbed transmission for the corresponding configuration.

5 Interpretation of the results

51 La Dôle—Mt-Pèlerin

The hop La Dôle—Mt-Pèlerin has to be considered as a special case since it is characterized by a pronounced lake reflection (τ = 110 ns). Because of its short length of only 54 km, it exhibits relatively few fading events. During the worst-month multipath propagation effects must be expected for 5 pc of the time. In such an interval the received level shows a Rayleigh distribution.

A fading with a depth of e. g. 20 dB then occurs with a probability of $0.05 \times 0.01 = 5 \cdot 10^{-4}$. Without lake reflections such fadings would be harmless because of its flat amplitude-frequency response as well as because of their frequency of occurrence. However, in combination with the lake reflections the transfer functions of figure 4 are unacceptable for any broadband digital transmission. An improvement of the transmission quality can be achieved, for example, by space-diversity reception tailored to the path geometry.

The interpretation of the results was therefore limited to the attenuation of the direct path. The analysis gave no sufficiently large amplitude variation in order to determine a significant delay between the two paths that produce the flat fading in all recorded fading events.

52 Chasseral—Albis

The hop Chasseral—Albis exhibits fadings during 50 pc of the time of the worst-month. This tenfold higher frequency of occurrence was expected by the d^3-law [5]. Also, the fact that the fading events show a very low selectivity is not surprising. The reason for this is certainly the knife-edge obstacle at 83 km (fig. 3) which suppresses dominating ground reflections.

For a large portion of the measured events it is therefore impossible to determine the parameters of a two-way or three-way model with sufficient accuracy. Instead it is precisely this relatively smooth amplitude response which suggests a polynomial approximation. A numerical analysis revealed that in most cases a second-order polynomial did suffice except only a few required polynomials of higher order ($\leqq 4$). This fact and the limitation of the human spatial imagination to three dimensions led to a preliminary restriction to the approximation with second-order polynomials. A later extension to polynomials of higher order or an approximation by the three-way model — if necessary and possible — is already foreseen in the computer programs.

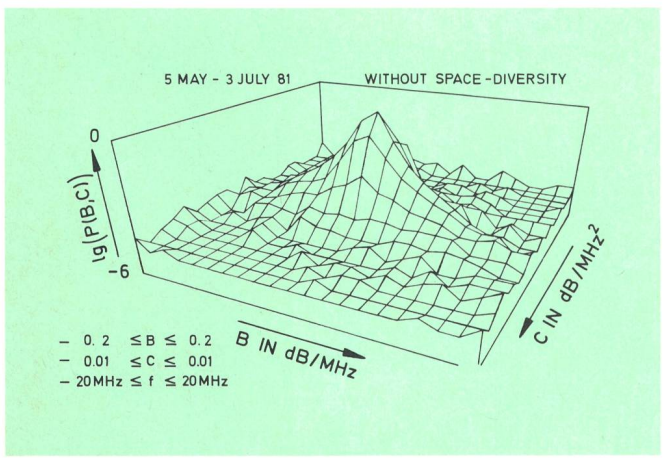

Fig. 7
Density function P (A, B, C) of the polynomial coefficients a, b and c
5 dB > a ≧ −45 dB (85 950 sweeps)

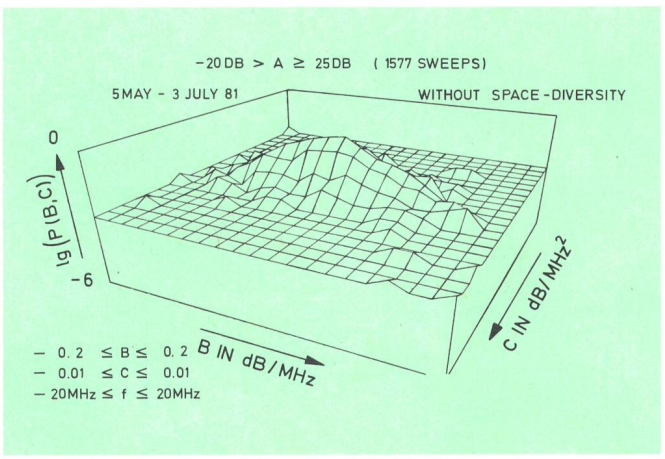

Fig. 8
Density function P (A, B, C) of the polynomial coefficients a, b and c
−20 dB > a ≧ −25 dB (1577 sweeps)

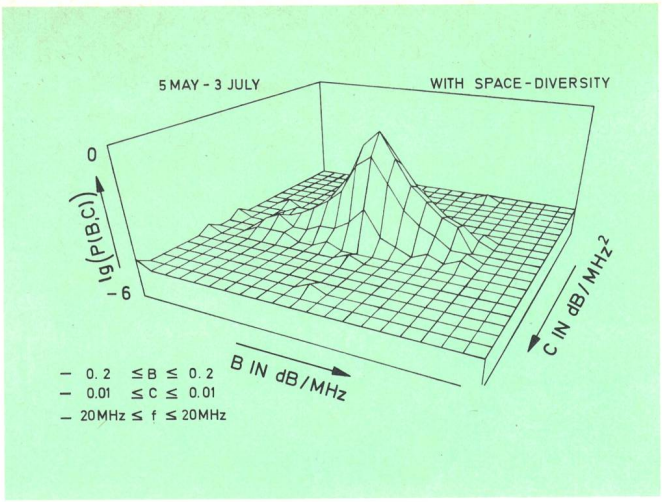

Fig. 9
Density function P (A, B, C) of the polynomial coefficients a, b and c
5 dB > a ≧ −45 dB (53 700 sweeps)

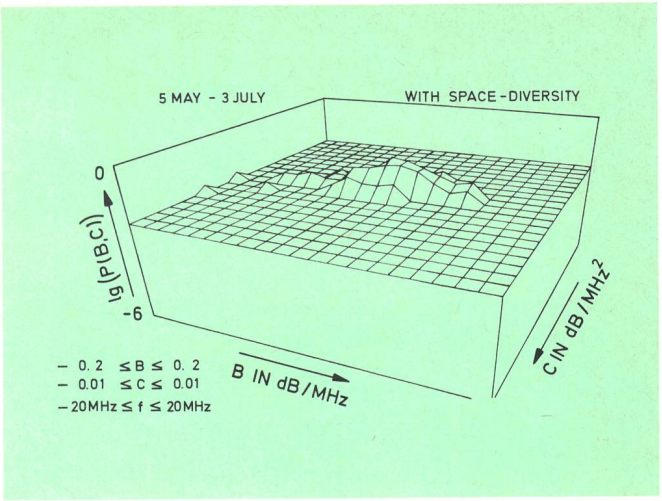

Fig. 10
Density function P (A, B, C) of the polynomial coefficients a, b and c
−20 dB > a ≧ −25 dB (146 sweeps)

The analysis of the transfer function was conducted in two steps. In a first step the three coefficients a, b, and c of the polynomial $a + bf + cf^2$ were determined for each swept measurement (40 measurement pairs of amplitude A_k and frequency f_k). This was done based on a least squares approximation. Each of the resulting triplets then represents an element of the density function matrix p (a, b, c), where the three quantities are assigned to 11 and 21 classes, respectively, in the intervals $+5 \geqq a \geqq -45$ dB, $-0.2 \leqq b \leqq 0.2$ dB/MHz, and $-0.01 \leqq c \leqq 0.01$ dB/MHz².

The logarithm of this density function p (a, b, c) can be plotted in three dimensions if one value, e. g. a, is kept constant. *Figure 7* shows lg p (a, b, c) for $+5 \geqq a \geqq -45$ dB, i. e. the frequency of occurrence of a pair of values (b, c) for an arbitrary value of a. Similarly, the values of lg p (a, b, c) can be drawn for smaller intervals of a, e. g. $-20 \geqq a \geqq -25$ dB *(fig. 8)*.

The improvement obtainable with space diversity reception is shown by the two probability functions of *figure 9* and *10* which can be compared directly with figure 7 and 8. On one side the frequency of occurrence of a deep fading is smaller and on the other side large values of |b| and |c| are less probable.

However, a direct comparison of numerical values only becomes possible after further processing. The figure 7 through 10 suggest to describe the function lg p (a, b, c), a = const. by a two-dimensional normal distribution.

$$p(b, c) = K \exp\left[-\frac{(b-\bar{b})^2}{2\tau_b^2} - \frac{(c-\bar{c})^2}{2\tau_c^2}\right]; \quad \bar{b} \simeq \bar{c} \simeq 0$$

The standard deviations σ_b and σ_c are thus a measure for the limits within which the coefficients b and c vary. It is quite reasonable to assume the variables b and c to be independent of each other, i. e. no correlation has to be taken into account. Thereby the estimation of the parameters of the distribution is also simplified; it follows directly from the marginal distribution.

6 Quantitative results

The approximation of the probability lg p (a, b, c), a = const. with a two-dimensional normal distribution, as explained in paragraph 52, leads to the value σ_b and σ_c. Both of these values are functions of the measure a that indicates the attenuation in the center of the channel. σ_b and σ_c are depicted in *figure 11* and *12* for both receiver configurations (with and without diversity reception).

From these figures it can be deduced that the linear and quadratic distortions increase linearly with fade depth to a first approximation. Diversity reception reduces this linear increase and the number of deep fading events. The relative cumulative probability for the occurrence of a particular attenuation a with and without diversity protection is shown in *figure 13*. The improvement factor

$$I = \frac{P\ (a, \text{without diversity protection})}{P\ (a, \text{with diversity protection})}$$

is in good agreement with that obtained in reference [6] by means of unmodulated carriers.

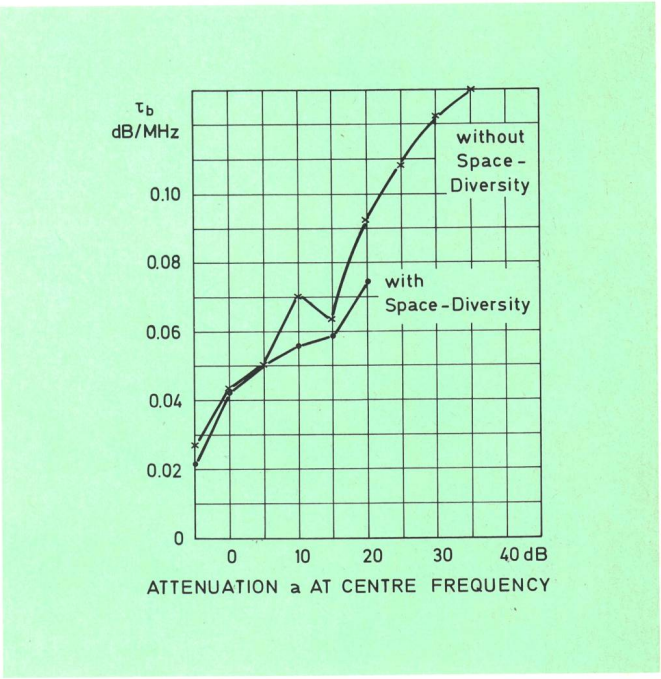

Fig. 11
Standard deviation τ_b (linear distortion) vs attenuation a at centre frequency

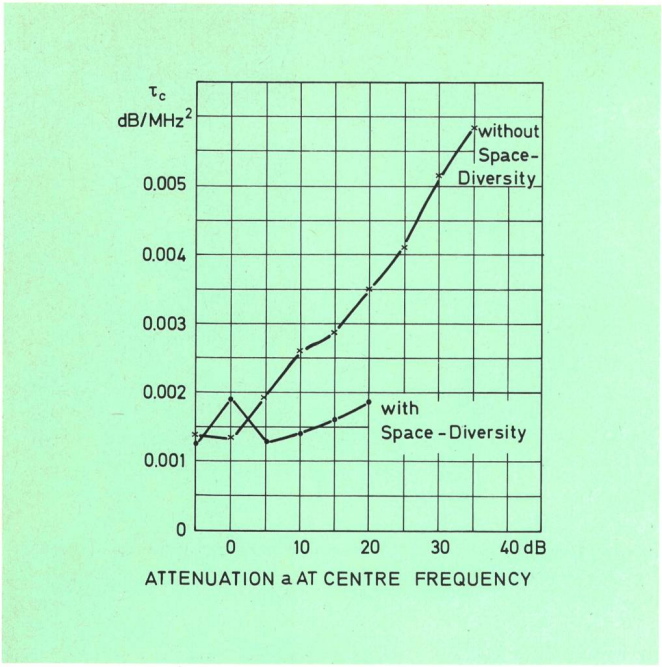

Fig. 12
Standard deviation τ_c (quadratic distortion) vs attenuation a at centre frequency

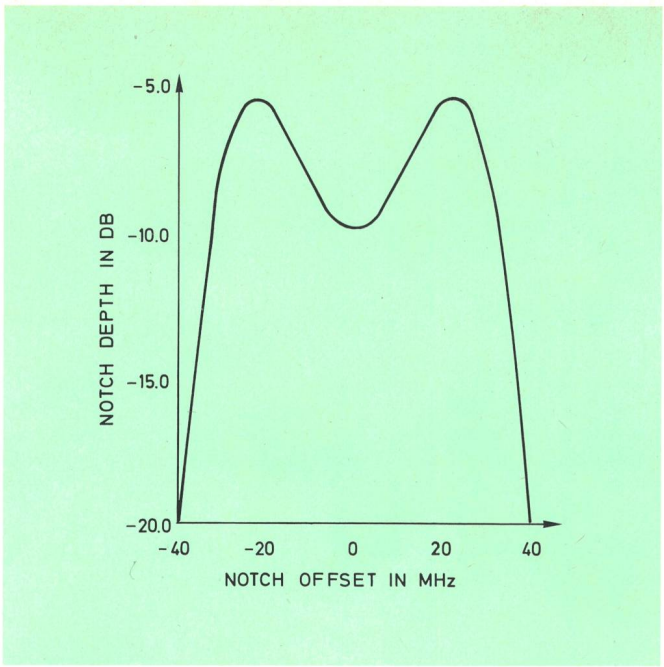

Fig. 14
Signature of a 90 Mbit/s 8 PSK digital radio system

7 Combination of equipment and propagation characteristics

The description of the propagation characteristics by means of polynomials cannot be compared directly with the usual description of equipment sensitivities by means of the signature. However, it is quite feasible to transform the signature from the original (λ, Δf)-space into the expanded polynomial space.

The signature of *figure 14* belongs to a 8PSK—90 Mbit/s system which results in the Boolean function in the image space as shown in *figure 15*. Inside of the curve the system operates error free [S(b, c) = 0], outside the transmission is disturbed [S(b, c) = 1].

The probability for a disturbed transmission on a particular hop can now be determined approximately by evaluating the expression

$$P\,(BER \geqq 10^{-3}) = \int\int S\,(b, c) \cdot p\,(b, c)\,db \cdot dc$$

To make this expression generally applicable, additional information is needed concerning the hop's dependence on the propagation characteristics. On the other hand some degree of clearness may have to be sacrified in favour of an approximation with higher-order polynomials, i. e. for both the signature S and the probability p, functions with more than two variables may have to be employed.

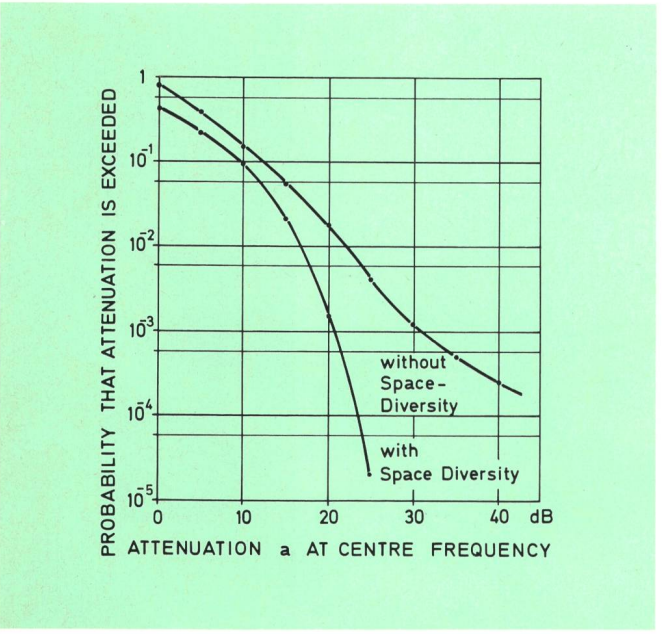

Fig. 13
Probability of attenuation a

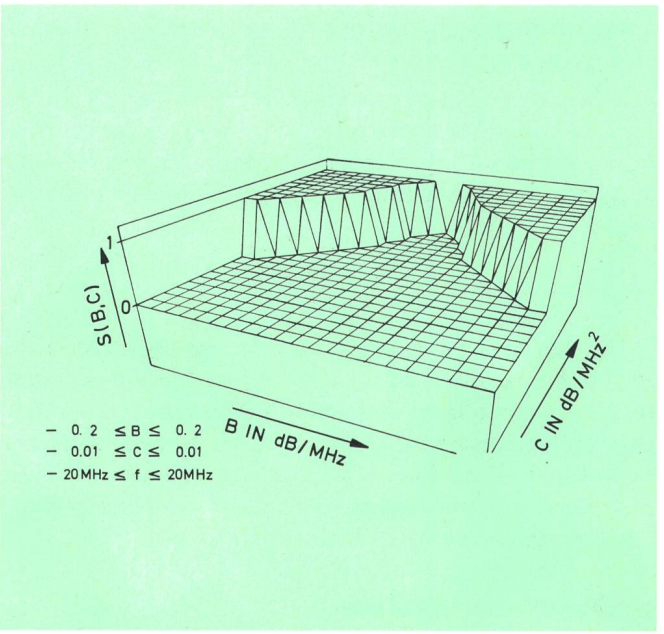

Fig. 15
Signature 90 Mbit/s 8 PSK mapped into the polynomial space

8 Conclusions

The model for the characterization of multipath propagation on line-of-sight hops must consist of at least three paths. In general, two of these differ by only small propagation delays and generate a flat attenuation. The third path, caused in many cases by a ground reflection, can be estimated based on the geometry of the profile and the nature of the ground.

The transmission improvement obtainable with space diversity reception is composed of the well-known improvement factor I and an additional reduction of the selectivity of the fadings.

The transfer function which is given by the propagation characteristics, and the signature of the equipment can both be defined in the expanded polynomial space. Thus an estimation of the outage time can be made.

References

[1] *Emshwiller M.* Characterization of the Performance of PSK Digital Radio Transmission in the Presence of Multipath Fading. Toronto, International Conference on Communications, 1978, 47.3.

[2] *Giger A. J.* and *Barnett W. T.* Effects of Multipath Propagation on Digital Radio. New York, IEEE Transactions on Communications, COM-29 (1981) 9.

[3] *Gysel U.* Elektronisches Raumdiversity-System für Richtfunkanlagen. München, NTG-Fachberichte Band 70 (1980), S. 199.

[4] *Rummer W. D.* Time- and Frequency-Domain Representation of Multipath Fading on Line-of-Sight Microwave Paths. Murray Hill, Bell System Technical Journal 59 (1980) 5, p. 763.

[5] *Vigants A.* Distance Variation of Two-Tone Amplitude Dispersion in Line-of-Sight Microwave Propagation. Denver, International Conference on Communications, 1981, 68.3.

[6] *Liniger M.* Dämpfungen auf Richtfunkverbindungen unter besonderer Berücksichtigung der Mehrwegausbreitung. Bern, Techn. Mitt. PTT 56 (1978) 5, S. 178 sowie Bell Translation Series TR 80—69.